State-space domain virtual point transformation for state-space identification in dynamic substructuring

R.S.O. Dias [1], **M. Martarelli** [1], **P. Chiariotti** [2]
[1] Università Politecnica delle Marche, Department of Industrial Engineering and Mathematical Sciences,
Via Brecce Bianche 12, 60131 Ancona, Italy
e-mail: **r.dasilva@staff.univpm.it**

[2] Politecnico di Milano, Department of Mechanical Engineering,
Via Privata Giuseppe La Masa 1, 20156 Milan, Italy

Abstract

In this article, the construction of state-space models suitable for dynamic substructuring (DS) applications is analysed in detail. The procedure derives the state-space model from the Frequency Response Functions (FRFs) measured on the components involved in the DS application. Moreover, a system identification algorithm is used to estimate the modal parameters from these FRFs. All the steps to properly construct a reliable state-space model by using the estimated modal parameters are presented and deeply analysed. Furthermore, the well-known Virtual Point Transformation (VPT) method is extended to the state-space domain. The approaches here discussed are validated by exploiting a set of FRFs collected from an experimental dynamic characterization of a mechanical system composed of two cross-shaped structures connected by a rubber mount. The paper demonstrates that the FRFs of the estimated state-space models very well-match the FRFs obtained by applying the VPT approach on the measured FRFs.

1 Introduction

During the last decades, dynamic substructuring (DS) has became a popular approach to characterize the dynamic behaviour of complex components. In literature, a wide variety of DS techniques can be found (see for example, [1],[2],[3],[4]). In this paper, we will focus our attention on the group of DS techniques tagged as State-Space Substructuring (SSS).

As the name suggests, the SSS techniques make use of state-space models to describe the dynamic behaviour of the components involved on the DS application. Thus, to use SSS methods we must start by identifying those state-space models. When the characterization of the substructures is performed by an experimental test, the estimation of the state-space models from the experimentally acquired data requires the use of system identification algorithms. In literature, we may find a wide variety of algorithms, for instance the subspace state-space algorithms, which are also commonly known as N4SID methods (see [5],[6],[7]), the PolyMAX method developed in [8] and the Maximum Likelihood Modal Parameter method (ML-MM) (see, [9]). In this article, to estimate state-space models from experimentally acquired data, the PolyMAX and ML-MM will be employed. These algorithms estimate modal parameters from a given set of measured FRFs. Then, by using those estimated modal parameters, state-space models can be constructed as reported in [10]. When estimating state-space models to be used in SSS applications, besides seeking for an excellent fit between the FRFs of the state-space models and the measured FRFs, the estimated models must also be physically consistent (see [3]). In this way, these models must be stable, must obey the second law of Newton and must be passive. Fortunately, by using PolyMAX and ML-MM algorithms, one makes sure that the estimated poles are stable (i.e. its real part is either zero or negative) and hence the estimated state-space models will be also stable. Nevertheless, these methods do not provide any guarantee that the estimated state-space models will always respect the second Newton's law nor that the estimated models are passive. In [11], an approach to force the estimated state-space models to respect the second Newton's law was suggested. This procedure will be used to force the estimated state-space models to obey the second Newton's law. The enforcement of passivity on the estimated state-space models lies beyond the scope of the present document.

SSS techniques also demand that the compatibility and equilibrium conditions (see [12]) are satisfied on the interfaces of the coupled components. Therefore, the estimated state-space models representative of the components involved on the DS application must present outputs and inputs placed on the interfaces of the connected substructures. In practice, this requirement can be hard to accomplish, because the interfaces might be inaccessible thus making the placement of sensors and/or actuators infeasible. To overcome this issue, it is common to apply the so-called Virtual Point Transformation (VPT) approach (see [13]). By assuming rigid local behaviour in the frequency band of interest, VPT enables the transformation of the outputs and inputs of the measured FRFs into the intended locations (i.e. the defined virtual points). In this way, the FRFs at the intended locations can be calculated. Then, from this set of FRFs the desired state-space models can be estimated.

The present article aims at providing a detailed description of the construction of state-space models by using modal parameters estimated from measured FRFs and to extend the VPT approach to the state-space domain.

The construction of state-space models from estimated modal parameters is analyzed in section 2. Then, in section 3 the VPT technique is extended to the state-space domain. In section 4 the approaches discussed in this paper are experimentally validated. Finally, in section 5 the conclusions are presented.

2 State-space models estimation

In this section, we will present how to compute a complete state-space model from the measured FRFs of an experimentally characterized mechanical system. Section 2.1 presents how to construct a state-space model from the modal parameters of the in-band modes. Then, in section 2.2 is presented how the contribution of the out-of-band modes can be represented in state-space model form. Afterwards, sections 2.3 and 2.4 present how to force a state-space model to respect the second law of Newton and how to construct the complete state-space model representative of the mechanical system under study, respectively.

2.1 In-band modes

To estimate the modal parameters from a set of measured FRFs, one must use a system identification method, for instance the PolyMAX [8] method and the Maximum Likelihood Modal Parameter method (ML-MM) [9]. From the obtained modal parameters, a modal model representative of the displacement FRFs of the mechanical system can be established as given by the following equation:

$$[H(j\omega)] = \sum_{r=1}^{n_m} \left(\frac{\{\psi_{ib,r}\}\{l_{ib,r}\}}{j\omega - \lambda_{ib,r}} + \frac{\{\psi_{ib,r}\}^*\{l_{ib,r}\}^*}{j\omega - \lambda^*_{ib,r}} \right) + \frac{[LR]}{(j\omega)^2} + [UR] \tag{1}$$

where, $[H(j\omega)] \in \mathbb{C}^{n_o \times n_i}$ is the FRF matrix, which presents n_o outputs and n_i inputs, n_m is the number of identified modes, subscript $[\bullet]^*$ denotes the complex conjugate of a matrix, $\{\psi_r\} \in \mathbb{C}^{n_o \times 1}$ is the r^{th} mode shape, $\{l_r\} \in \mathbb{C}^{1 \times n_i}$ is the r^{th} modal participation factor, λ_r is the r^{th} pole, $[LR] \in \mathbb{R}^{n_o \times n_i}$ and $[UR] \in \mathbb{R}^{n_o \times n_i}$ are the lower and upper residuals matrices, whose function is modelling respectively the influence of the lower and upper out-of-band modes in the considered frequency band. Finally, subscript ib denotes vectors/matrices associated to the in-band modes.

By following [14], the modal model given by equation (1) can be rewritten as follows:

$$[H(j\omega)] = [\Psi_{ib} \quad \Psi^*_{ib}] \left[j\omega[I] - \begin{bmatrix} \Lambda_{ib} & 0 \\ 0 & \Lambda^*_{ib} \end{bmatrix} \right]^{-1} \begin{bmatrix} L_{ib} \\ L^*_{ib} \end{bmatrix} + \frac{[LR]}{(j\omega)^2} + [UR] \tag{2}$$

where, $[\Lambda] \in \mathbb{C}^{n_m \times n_m}$ is a diagonal matrix that contains the system poles, $[L] \in \mathbb{C}^{n_m \times n_i}$ is the modal participation matrix and $[\Psi] \in \mathbb{C}^{n_o \times n_m}$ is the mode shape matrix.

From the well-known expression to calculate the FRFs of a state-space model (see [14]), equation (2) can be rewritten as follows

$$[H(j\omega)] = [C_{ib}](j\omega[I] - [A_{ib}])^{-1}[B_{ib}] + \frac{[LR]}{(j\omega)^2} + [UR] \tag{3}$$

where, matrices $[A_{ib}]$, $[B_{ib}]$ and $[C_{ib}]$ are given in expression (4).

$$[A_{ib}] = \begin{bmatrix} \Lambda_{ib} & 0 \\ 0 & \Lambda_{ib}^* \end{bmatrix}, \quad [B_{ib}] = \begin{bmatrix} L_{ib} \\ L_{ib}^* \end{bmatrix}, \quad [C_{ib}] = [\Psi_{ib} \quad \Psi_{ib}^*] \tag{4}$$

2.2 Out-of-band modes

The contribution of the out-of-band modes may be significant, therefore the inclusion of the upper and lower residual matrices is fundamental in order to obtain a complete state-space model representative of the system under study. In this way, in the following subsections we will analyze how they can be represented in state-space model form. The procedures that will be here presented were proposed in [10].

2.2.1 Upper residual matrix

To take into account the contribution of the upper residual matrix, residual compensation modes (RCMs) will be computed from its singular value decomposition (SVD). By performing the SVD of the upper residual matrix, we obtain:

$$[UR] = [U_{UR}][\sigma_{UR}][V_{UR}]^T = \sum_{r=1}^{n_{UR}} \{U_{UR,r}\}\sigma_{UR,r}\{V_{UR,r}\}^T \tag{5}$$

where, $[U_{UR}] \in \mathbb{R}^{n_o \times n_{UR}}$ and $[V_{UR}] \in \mathbb{R}^{n_{UR} \times n_i}$ are the matrices composed by the left and right eigenvectors of matrix $[UR]$, respectively, whereas $[\sigma_{UR}] \in \mathbb{R}^{n_{UR} \times n_{UR}}$ is a diagonal matrix composed by the singular values of $[UR]$ [15]. Subscript UR denotes vectores/matrices associated to the upper residual matrix, while $n_{UR} = min(n_i, n_o)$.

By adopting a proportional damping modal model, for which the residue matrices (i.e. $[R_r]$=$\{\psi_r\}\{l_r\}$) are pure imaginary [9], the upper residual matrix can be approximated as follows:

$$[UR] \approx [H_{UR}(j\omega)] = \sum_{r=1}^{n_{UR}} \left(\frac{2j\omega_{UR,r}\sqrt{1-\xi_{UR,r}^2}}{(j\omega)^2 + 2j\omega\xi_{UR,r}\omega_{UR,r} + \omega_{UR,r}^2}\{\psi_{UR,r}\}\{l_{UR,r}\} \right) \tag{6}$$

where, $\omega_{UR,r}$ and $\xi_{UR,r}$ are the chosen natural frequency and the damping ratio of the r^{th} mode of the computed RCMs, respectively. Vectors $\{\psi_{UR,r}\}$ and $\{l_{UR,r}\}$ are given by expressions (7a) and (7b).

$$\{\psi_{UR,r}\} = \frac{\omega_{UR,r}}{\sqrt{1-\xi_{UR,r}^2}}\sqrt{\sigma_{UR,r}}\{U_{UR,r}\} \tag{7a}$$

$$\{l_{UR,r}\} = -\frac{j}{2}\sqrt{\sigma_{UR,r}}\{V_{UR,r}\}^T \tag{7b}$$

By using equations (7a) and (7b) with equation (6), one can conclude that equations (5) and (6) match at $\omega = 0 \; rads^{-1}$. To conclude this subsection, we must reflect on the selection of the natural frequencies and damping ratios of the computed RCMs. For the sake of simplicity, let us assume that all the natural frequencies and all the damping ratios of the RCMs are chosen to be equal (which is a common choice). Hence, for $\omega = 0\ rads^{-1}$ and by using equation (6), we may establish the equality given by equation (8).

$$[UR] = [H_{UR}(0)] = \frac{\sum_{r=1}^{n_{UR}} \left(2j\omega_{UR}\sqrt{1-\xi_{UR}^2}\{\psi_{UR,r}\}\{l_{UR,r}\}\right)}{\omega_{UR}^2} \tag{8}$$

By mathematically manipulating equation (8), we arrive to the expression given below.

$$\sum_{r=1}^{n_{UR}} \left(2j\omega_{UR}\sqrt{1-\xi_{UR}^2}\{\psi_{UR,r}\}\{l_{UR,r}\}\right) = \omega_{UR}^2[UR] \tag{9}$$

By observing equations (6) and (9) it is straightforward that the higher the frequency ω_{UR} and the lower the damping ratio ξ_{UR}, the more accurate the proportional damping modal model (see equation (6)) will be to approximate the contribution of the upper residual matrix. Nevertheless, if the constructed state-space model is intended to be used for time-domain simulations, $\xi_{UR} = 0$ must not be selected, because undamped modes may lead to instabilities as reported in [10]. On the other hand, in general it should be $5 \times \omega_{max} \leq \omega_{UR}$ (where ω_{max} is the maximum frequency of interest) [10].

From the estimated RCMs, a state-space model representative of the upper residual matrix can be defined as follows:

$$\begin{aligned} \{\dot{x}_{UR}(t)\} &= [A_{UR}]\{x_{UR}(t)\} + \left[B_{UR}\right]\{u_{UR}(t)\} \\ \{y_{UR}(t)\} &= \left[C_{UR}\right]\{x_{UR}(t)\} \end{aligned} \tag{10}$$

where, the value of its state-space matrices are given below.

$$[A_{UR}] = \begin{bmatrix} \Lambda_{UR} & 0 \\ 0 & \Lambda_{UR}^* \end{bmatrix}, \quad [B_{UR}] = \begin{bmatrix} L_{UR} \\ L_{UR}^* \end{bmatrix}, \quad [C_{UR}] = [\Psi_{UR} \quad \Psi_{UR}^*] \tag{11}$$

Where, matrix $[\Lambda_{UR}]$ is a diagonal matrix composed by the poles of the RCMs, which are calculated by following the expression given below.

$$\lambda_{UR}, \lambda_{UR}^* = -\xi_{UR}\omega_{UR} \pm j\omega_{UR}\sqrt{1-\xi_{UR}^2} \tag{12}$$

2.2.2 Lower residual matrix

To take into account the contribution of the lower residual matrix a proportional damping modal model will be again employed. However, we are now seeking to approximate the contribution of a frequency dependent matrix $\left[-\frac{LR}{\omega^2}\right]$ (see equation (3)), for this reason it is not clear which matrix must be used to compute the RCMs needed to construct the proportional damping modal model. To better assess this question, let us consider a generic proportional damping modal model as follows:

$$-\frac{[LR]}{\omega^2} \approx [H_{LR}(j\omega)] = \sum_{r=1}^{n_{LR}} \left(\frac{2j\omega_{LR,r}\sqrt{1-\xi_{LR,r}^2}}{(j\omega)^2 + 2j\omega\xi_{LR,r}\omega_{LR,r} + \omega_{LR,r}^2}\{\psi_{LR,r}\}\{l_{LR,r}\} \right) \tag{13}$$

where, subscript LR denotes vectors/matrices associated to the lower residual matrix, while $n_{LR} = min(n_i, n_o)$.

By observing equation (13), we may conclude that the proportional modal model will represent a good approximation of the contribution of $\left[-\frac{LR}{\omega^2}\right]$, if its numerator is equal to $[LR]$ and if the natural frequencies of the RCMs present very small values. Let us once again suppose that all the natural frequencies and all the damping ratios of the computed RCMs are selected to be equal. By making the referred assumption, for $\omega = 0\ rads^{-1}$ equation (13) may be rewritten as given below.

$$[H_{LR}(0)] = \frac{\sum_{r=1}^{n_{LR}} \left(2j\omega_{LR}\sqrt{1-\xi_{LR}^2}\{\psi_{LR,r}\}\{l_{LR,r}\}\right)}{\omega_{LR}^2} \tag{14}$$

As mentioned, we aim at constructing a modal model, whose numerator is equal to $[LR]$, thus by observing equation (14) we conclude that $[H_{LR}(0)]$ must be equal to $\left[\frac{LR}{\omega_{LR}^2}\right]$. Hence, the RCMs must be set up from the modal parameters estimated through the SVD of $\left[\frac{LR}{\omega_{LR}^2}\right]$. By analysing equations (13) and (14), we may also conclude that as we select smaller values for ω_{LR} and ξ_{LR}, more accurate becomes the proportional damping modal model to replicate the contribution of $\left[-\frac{LR}{\omega^2}\right]$. As rule of thumb, the value of ω_{LR} must be selected to respect $\omega_{LR} \leq \frac{1}{5}\omega_{min}$ (where ω_{min} is the minimum frequency of interest), while the value of ξ_{LR} must be selected to be greater than zero if time-domain simulations are intended to be performed with the estimated state-space model [10]. The computation of the RCMs representative of the lower out-of-band modes follows the described procedures to compute the RCMs representative of the upper out-of-band ones (see section 2.2.1). From the estimated RCMs, a state-space model representative of $\left[-\frac{LR}{\omega^2}\right]$ can be defined in a similar way as reported for the $[UR]$ matrix (see equations (10), (11) and (12)).

2.3 Imposing the Newton's second law

One of the criteria that the constructed state-space models must obey in order to be physically consistent is the Newton's second law. This physical law states that there exists a direct relation between force and acceleration, not existing direct relations between force and displacement or velocity. This means that the feedthrough matrix of displacement and velocity state-space models (state-space models whose output vectors are composed by displacement and velocities, respectively) must be null. This condition is always fulfilled by the displacement state-space models (since $[D] = [0]$, see equation (2)), while the same does not necessarily hold for velocity ones. To better demonstrate this fact, let us differentiate expression (3) in order to obtain a velocity state-space model and its respective FRFs, as follows:

$$j\omega[H(j\omega)] = [C_{ib}][A_{ib}](j\omega[I] - [A_{ib}])^{-1}[B_{ib}] + [C_{ib}][B_{ib}] + \frac{[LR]}{j\omega} + j\omega[UR] \tag{15}$$

Observing equation (15), we can identify the state-space matrices of the velocity state-space model:

$$[A_{ib}^{vel}] = [A_{ib}], \quad [B_{ib}^{vel}] = [B_{ib}], \quad [C_{ib}^{vel}] = [C_{ib}][A_{ib}], \quad [D_{ib}^{vel}] = [C_{ib}][B_{ib}] \tag{16}$$

where, superscript vel denotes vectors/matrices associated to a velocity state-space model.

From expressions (15) and (16), one may conclude that, indeed, we do not have any guarantee that $[D^{vel}]$ will be a null matrix. Besides making the state-space model violate the second law of Newton, the computation of a state-space model, whose $[D^{vel}] \neq [0]$ has negative practical effects. Firstly, it unables the proper transformation of the state-space models into coupling form (for details see [3]), which disables the computation of minimal order models when coupling/decoupling state-space models that are not established in the physical domain (e.g. models identified from experimentally acquired data). Secondly, it promotes a bias between the accelerance FRF of the modal model and the FRFs of the constructed acceleration state-space model. To demonstrate the second negative effect, let us differentiate equation (15) in order to obtain an acceleration state-space model and its respective FRFs, as follows:

$$(j\omega)^2[H(j\omega)] = [C_{ib}][A_{ib}][A_{ib}](j\omega[I] - [A_{ib}])^{-1}[B_{ib}] + [C_{ib}][A_{ib}][B_{ib}] + j\omega[C_{ib}][B_{ib}] + [LR] + (j\omega)^2[UR] \tag{17}$$

where, we can identify the state-space matrices of the acceleration state-space model as given below.

$$[A_{ib}^{accel}] = [A_{ib}], \quad [B_{ib}^{accel}] = [B_{ib}], \quad [C_{ib}^{accel}] = [C_{ib}][A_{ib}][A_{ib}], \quad [D_{ib}^{accel}] = [C_{ib}][A_{ib}][B_{ib}] \tag{18}$$

Expressions (17) and (18) clearly demonstrate that the term $j\omega[C_{ib}][B_{ib}]$ is not taken in account when constructing the acceleration state-space model. Hence, if this term is not null, a bias between the accelerance FRFs of the modal model and of the state-space model will be observed. Before presenting a solution to guarantee that $[C_{full}][B_{full}] = [0]$ (where, subscript $full$ denotes matrices/vectors associated to the complete state-space model) is verified, we must better understand in which situations this product is null and in which it is not. To perform such reasoning let us develop the product $[C_{ib}][B_{ib}]$ by using the value of both matrices given in equation (4).

$$[C_{ib}][B_{ib}] = [\Psi_{ib} \quad \Psi_{ib}^*] \begin{bmatrix} L_{ib} \\ L_{ib}^* \end{bmatrix} = [\Psi_{ib} L_{ib} + \Psi_{ib}^* L_{ib}^*] \tag{19}$$

By analyzing equation (19), we understand that if our modal model is constructed by assuming proportional damping, $[C_{ib}][B_{ib}] = [0]$. This statement holds for proportionally damped systems, because the product $[\Psi_{ib}][L_{ib}]$ would be pure imaginary (see equations (7a) and (7b)). Therefore, the state-space models representative of both upper and lower out-of-band modes will verify $[C_{UR,LR}][B_{UR,LR}] = [0]$, provided that the computed RCMs are assumed to be under-damped (i.e. ξ_{UR} and ξ_{LR} are selected to be smaller than 1). Note also that, if a modal model is constructed without assuming proportional damping, matrix $[C_{ib}][B_{ib}]$ will always be real.

In general, real mechanical systems do not present a proportional damping, hence $[C_{ib}][B_{ib}] \neq [0]$ is usually verified. Thus, it is fundamental to figure out a procedure to make sure that $[C_{full}][B_{full}]$ is null. A possible solution is the computation of RCMs that are able to include the contribution of $[C_{ib}][B_{ib}]$ into the complete velocity state-space model and at same time that impose $[C_{full}][B_{full}] = [0]$. However, the inclusion of those RCMs should be performed directly on the displacement state-space model, because it is simple to calculate both velocity and acceleration models from it, whereas going from the velocity or acceleration model to the displacement one involves the inversion of state-space matrices (see expressions (16) and (18)), which may introduce ill-conditioned matrix inversions.

The modal parameters required to compute the intended RCMs must be obtained from the SVD of $[C_{ib}][B_{ib}]$ matrix as follows

$$[C_{ib}][B_{ib}] = [U_{CB}][\sigma_{CB}][V_{CB}]^T = \sum_{r=1}^{n_{CB}} \{U_{CB,r}\}\sigma_{CB,r}\{V_{CB,r}\}^T \tag{20}$$

where, $[U_{CB}] \in \mathbb{R}^{n_o \times n_{CB}}$ and $[V_{CB}] \in \mathbb{R}^{n_{CB} \times n_i}$ are the matrices composed by the left and right eigenvectors of matrix $[C_{ib}][B_{ib}]$, respectively, whereas $[\sigma_{CB}] \in \mathbb{R}^{n_{CB} \times n_{CB}}$ is a diagonal matrix composed by the singular values of $[C_{ib}][B_{ib}]$ [15]. Subscript CB denotes vectores/matrices associated to the $[C_{ib}][B_{ib}]$ matrix, while $n_{CB} = min(n_i, n_o)$.

By following the approach reported in [11] and having in mind that $[C_{ib}][B_{ib}]$ is real, the state-space model of the RCMs used to impose $[C_{full}][B_{full}] = [0]$, must be computed as follows.

$$[A_{CB}] = \begin{bmatrix} j\omega_{CB,1} & & \\ & \ddots & \\ & & j\omega_{CB,n_{CB}} \end{bmatrix} \quad [B_{CB}] = \begin{bmatrix} -\sqrt{\sigma_{CB,1}}V_{CB,1}^T \\ \vdots \\ -\sqrt{\sigma_{CB,n_{CB}}}V_{CB,n_{CB}}^T \end{bmatrix} \quad [C_{CB}] = \begin{bmatrix} U_{CB,1}\sqrt{\sigma_{CB,1}} \\ \vdots \\ U_{CB,n_{CB}}\sqrt{\sigma_{CB,n_{CB}}} \end{bmatrix}^T \tag{21}$$

Let us assume that the state-space model intended to be constructed presents a single input and output (SISO). By computing the FRF of the displacement state-space model of the RCM used to impose $[C_{full}][B_{full}] = [0]$, we obtain the expression given bellow.

$$[H_{CB}(j\omega)] = -\frac{U_{CB}\sigma_{CB}V_{CB}^{T}}{j\omega - j\omega_{CB}} \tag{22}$$

As the contribution of $[C_{ib}][B_{ib}]$ is null for the complete displacement state-space model, we intend that $[H_{CB}(j\omega)]$ be as close to null as possible. Thus, it is straightforward that as larger gets ω_{CB} more accurate is the RCM to fulfill the mentioned requirement. However, for both velocity and acceleration state-space models, the contribution of $[C_{ib}][B_{ib}]$ is not null (see equations (15) and (17)). To better understand how the computed RCM compensates the contribution of this term into both velocity and acceleration models, it is sufficient to observe the FRF of the velocity state-space model of the RCM as follows

$$j\omega[H_{CB}(j\omega)] = \frac{-\omega_{CB}U_{CB}\sigma_{CB}V_{CB}^{T}}{\omega - \omega_{CB}} - U_{CB}\sigma_{CB}V_{CB}^{T} \tag{23}$$

where, the first term on the right side of equations (23) has the function of including the contribution of $[C_{ib}][B_{ib}]$ into the complete velocity state-space model, while the second term of the same equation imposes that $[C_{full}][B_{full}] = [0]$. Hence, we may conclude that as larger gets ω_{CB} more close to $[C_{ib}][B_{ib}]$ will be the value of the first term on the right side of the equation (as intended). Therefore, once again we conclude that as we select a larger value of ω_{CB} to set up the RCM more accurate it will be. Note that, even though we have analyzed a SISO system to demonstrate that the RCMs are more accurate as ω_{CB} is selected to be greater, the same relation holds for multiple input and multiple output (MIMO) systems.

As final note, we must alert the readers that including undamped RCMs into the complete state-space model is not recommended, when it is intended to perform time-domain simulations with the estimated state-space model [10]. For this reason, if time-domain simulations are intended to be performed, it is suggested to estimate the modal model from the measured FRFs by assuming a proportionally damped model. The computation of such a model is possible, for instance, by following the procedure presented in [9], in this way we ensure that $[C_{ib}][B_{ib}] = [0]$. However, for mechanical systems that are not suitable to be modelled by a proportionally damped modal model, one should be prepared for the possibility of obtaining a lower quality match between the computed modal model and the set of FRFs, when compared to the quality of the match if a proportionally damped modal model would not be assumed.

2.4 Construction of the complete state-space model

After calculating the state-space models representative of the in-band modes (see section 2.1), of the upper and lower out-of-band modes (see sections 2.2.1 and 2.2.2, respectively) and of the RCMs computed from $[C_{ib}][B_{ib}]$ (see section 2.3) a complete displacement state-space model can be established as follows

$$\begin{aligned} \{\dot{x}_{full}(t)\} &= [A_{full}]\{x_{full}(t)\} + \left[B_{full}\right]\{u_{full}(t)\} \\ \{y_{full}(t)\} &= \left[C_{full}\right]\{x_{full}(t)\} \end{aligned} \tag{24}$$

where, the value of its state-space matrices are given by the following expression:

$$[A_{full}] = \begin{bmatrix} \Lambda_{ib,LR,UR} & 0 & 0 \\ 0 & \Lambda_{ib,LR,UR}^{*} & 0 \\ 0 & 0 & A_{CB} \end{bmatrix}, \quad [B_{full}] = \begin{bmatrix} L_{ib,LR,UR} \\ L_{ib,LR,UR}^{*} \\ B_{CB} \end{bmatrix}, \quad [C_{full}] = \begin{bmatrix} \Psi_{ib,LR,UR} \\ \Psi_{ib,LR,UR}^{*} \\ C_{CB} \end{bmatrix}^{T} \tag{25}$$

where, matrices $[\Lambda_{ib,LR,UR}]$, $[L_{ib,LR,UR}]$ and $[\Psi_{ib,LR,UR}]$ are given below.

$$[\Lambda_{ib,LR,UR}] = \begin{bmatrix} \Lambda_{i_b} & 0 & 0 \\ 0 & \Lambda_{LR} & 0 \\ 0 & 0 & \Lambda_{UR} \end{bmatrix}, \quad [L_{ib,LR,UR}] = \begin{bmatrix} L_{i_b} \\ L_{LR} \\ L_{UR} \end{bmatrix}, \quad [\Psi_{ib,LR,UR}] = [\Psi_{i_b} \quad \Psi_{LR} \quad \Psi_{UR}] \tag{26}$$

3 Extending VPT approach to the state-space domain

Let us assume that by experimentally characterizing a mechanical system, whose interfaces were inaccessible to place sensors and to be properly excited, the following set of FRFs was measured

$$[H_{MD}(j\omega)] = \frac{\{Y(j\omega)\}}{\{U(j\omega)\}} \tag{27}$$

where, $\{Y(j\omega)\}$ is the set of measured responses/outputs, $[H_{MD}(j\omega)]$ represents the set of measured FRFs and $\{U(j\omega)\}$ represents the excitation/inputs. Let us now further assume that this mechanical system will be used in a DS application, hence we are required to obtain its FRFs at the interfaces. To obtain the FRFs at the intended locations and provided that the component behaves as a rigid body in the frequency band of interest, we may apply the VPT approach. By using this approach, we must transform the outputs and inputs of the measured set of FRFs given by equation (27) into the intended locations (i.e. into the defined virtual points) as follows

$$\{Q(j\omega)\} = [T_y][H_{MD}(j\omega)][T_u]^T\{M(j\omega)\} \tag{28}$$

where, $\{Q(j\omega)\}$ represents the set of responses/outputs at the virtual points (VPs) location and $\{M(j\omega)\}$ represents the VPs forces, while matrices $[T_y]$ and $[T_u]^T$ are given below.

$$[T_y] = (R_y^T R_y)^{-1} R_y^T \tag{29a}$$

$$[T_u]^T = R_u(R_u^T R_u)^{-1} \tag{29b}$$

where, matrices R_y and R_u must be computed as reported in [13].

Assuming that from $[H_{MD}(j\omega)]$ and by using the procedures presented in 2, a state-space model was identified, we have:

$$\begin{aligned} \{\dot{x}(t)\} &= [A_{MD}]\{x(t)\} + \left[B_{MD}\right]\{u(t)\} \\ \{y(t)\} &= \left[C_{MD}\right]\{x(t)\} \end{aligned} \tag{30}$$

by calculating the FRFs of the state-space model given by expression (30) (see [14]), equation (28) can be rewritten as follows.

$$\{Q(j\omega)\} = [T_y]\left([C_{MD}](j\omega[I] - [A_{MD}])^{-1}[B_{MD}]\right)[T_u]^T\{M(j\omega)\} \tag{31}$$

By observing equation (31), we conclude that from the state-space model given in expression (30), we may derive a state-space model, whose outputs are the VPs responses and the inputs are the VPs forces. The state-space matrices of this model can be calculated as given below.

$$[A_{VP}] = [A_{MD}], \quad [B_{VP}] = [B_{MD}][T_u]^T, \quad [C_{VP}] = [T_y][C_{MD}] \tag{32}$$

It is worth mentioning that one can estimate a state-space model representative of the FRFs placed at the defined VPs by firstly applying VPT on the measured FRFs and then by estimating the state-space model representative of the FRFs at the defined VPs. However, if at the end of this process the user notices a mistake, for instance on the $[R_y]$ and/or $[R_u]$ matrices, the full procedure will have to be repeated. Conversely, by following the approach here described, if the user finds an error on the computation of the $[R_y]$ and/or $[R_u]$, this mistake can be easily fixed, because a state-space model representative of the measured FRFs is available. For this reason, one is just required to fix the transformation matrices and recalculate the state-space model representative of the FRFs at the VPs locations in accordance with equation (31). The mentioned advantage of the approach here described is substantial, because the estimation of state-space models representative of experimentally acquired FRFs is usually a time consuming task.

4 Experimental validation

4.1 Testing campaign

To experimentally validate the approaches here discussed, a structure composed by two steel crosses connected by a rubber mount (from now on denoted as Assembly Steel) was tested (see figure 1).

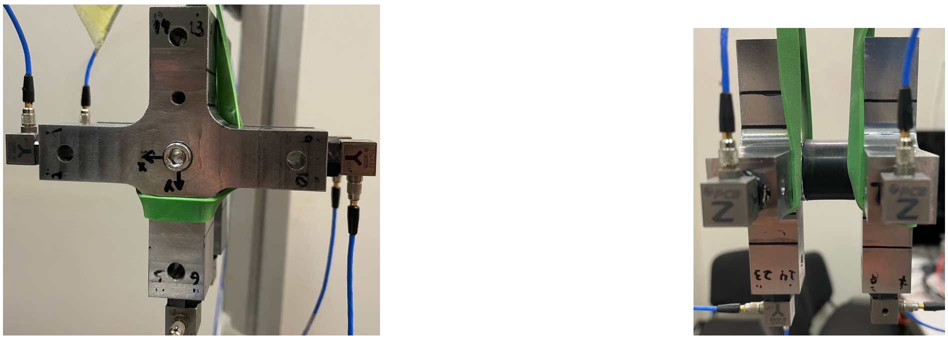

(a) Front perspective. (b) Side perspective.

Figure 1: Structure composed by two steel crosses connected by a rubber mount.

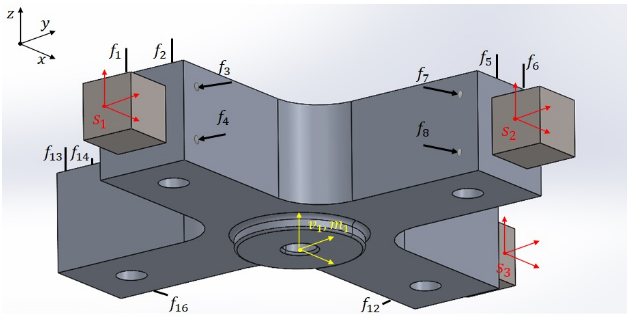

Figure 2: Locations of measurement accelerometers (red), hammer impact directions (black arrows) and virtual point (yellow) [16].

Every SSS method requires the use of state-space models, whose outputs and inputs are placed at the interface of the structures involved in the DS application. Thus, we seek to obtain a state-space model representative of the structure under analysis, whose outputs and inputs are placed at the interface of each cross with the rubber mount. However, the placement of sensors or actuators at those locations is infeasible. For this reason, the crosses were designed to behave as rigid bodies in the frequency range of interest, which was defined to be between 20 Hz and 500 Hz.

The roving hammer testing approach was used to experimentally characterize the structure shown in figure 1. Each steel cross was instrumented with three accelerometers (PCB Model TLD356A32), while the model of the used hammer is PCB 086C03. Hammer hits were provided at sixteen different locations (see figure 2). The cross shapes were designed to guarantee an effective excitation of the rotational DOFs. In this way, a reliable twelve DOFs characterization of the structure under test was possible (see [17], [18]).

4.2 Identified state-space models

Two different state-space models were computed out of the experimental data collected during the testing campaign described in section 4.1. The first one was obtained by applying VPT on the measured set of FRFs, then a state-space model was computed from the obtained FRFs by following the procedures outlined in section 2. The second one was obtained by estimating a state-space model representative of the measured FRFs (see section 2) and applying VPT to transform the outputs and inputs of the estimated state-space models to the intended locations (from now on this approach will be denoted as VPT-SS). It is important to mention that to estimate the modal parameters from the FRFs, the Simcenter Testlab® implementation of the PolyMAX and ML-MM methods was exploited. Furthermore, during the estimation of the modal parameters it was not assumed a proportional damped model, hence it is expected that $[C_{ib}][B_{ib}] \neq [0]$. To compute the RCMs, we have initially selected their natural frequencies to be: $\omega_{LR} = 0.1$ Hz, $\omega_{UR} = 15000$ Hz and $\omega_{CB} = 50000$ Hz. However, it was verified that for the state-space model directly estimated from the FRFs obtained by applying VPT approach on the measured FRFs the contribution of $j\omega[C_{ib}][B_{ib}]$ to the acceleration state-space model (see equation (17)) was not properly compensated. Therefore, to compute this state-space model was selected $\omega_{CB} = 500000$ Hz. Furthermore, the computed RCMs to compensate the contribution of the out-of-band modes were selected to be undamped, in order to obtain the best possible match between the FRFs of the estimated state-space models and the FRFs obtained by applying the VPT approach on the measured FRFs. The comparison of two FRFs of both estimated state-space models with the correspondent FRFs obtained by applying VPT on the measured FRFs is provided in figures 3. It is worth to mention that in the caption of figures 3 and through the rest of the article, the virtual point outputs of the rightmost cross in figure 1b will be denoted as v_1, while the VP outputs of the leftmost cross (see figure 1b) will be labelled as v_2. On the other hand, the VP inputs of the rightmost cross in figure 1b will be tagged as m_1, while the VP outputs of the leftmost cross (see figure 1b) will be denoted as m_2.

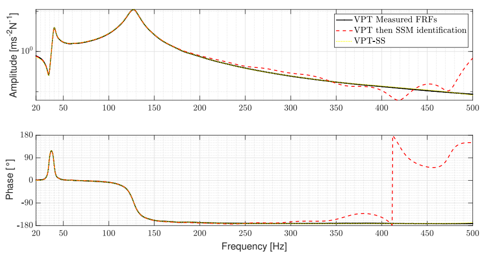

(a) Accelerance FRF of the Assembly Steel, whose output is the DOF v_1^y and the input is the DOF m_2^y.

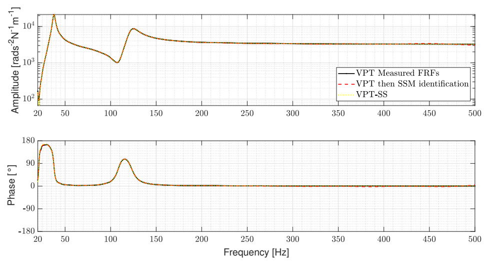

(b) Accelerance FRF of the Assembly Steel, whose output is the DOF $v_2^{R_y}$ and the input is the DOF $m_2^{R_y}$.

Figure 3: Comparison of the FRFs obtained by applying VPT on the measured FRFs (reference FRFs, black) with the same FRFs of the state-space models obtained directly from the transformed FRFs (red) and by exploiting VPT-SS approach (yellow).

By observing figures 3, we may conclude that the FRFs of the state-space model obtained by VPT-SS very well match those obtained by applying VPT approach on the measured FRFs (reference FRFs). The driving point FRF of the state-space model directly estimated from the FRFs obtained by applying VPT approach on the measured FRFs very well match the reference FRF (see figure 3b), while the FRF of the same state-space model presented in figure 3a very well-match the reference FRF only up to 350 Hz. Furthermore, the number of in-band modes used to set up this state-space model was 82, while 147 modes were used to set up the model directly estimated from the VP-transformed FRFs. This fact may represent an important decrease on the computational cost, when performing calculations with the state-space model obtained by VPT-SS approach instead with the one directly estimated from the FRFs obtained by applying VPT on the experimentally measured FRFs. It is worth mentioning that the structure under analysis (see figure 1) does not present so many modes in the frequency band of interest. However, we are seeking for the best possible fit between the FRFs of the estimated state-space models and the measured FRFs, which lead to the construction of state-space models by including a large amount of modes.

To demonstrate that the procedures presented in sections 2.2 and 2.3 are also valid to compute damped RCMs, VPT-SS was again used to estimate the intended state-space model, however this time the RCMs responsible for compensating the contribution of the out-of-band modes were assumed to present a damping ratio of 10%. In figure 4 is presented the comparison of two FRFs obtained by applying VPT on the measured FRFs with the same FRFs of the state-space models obtained by using VPT-SS and by including undamped

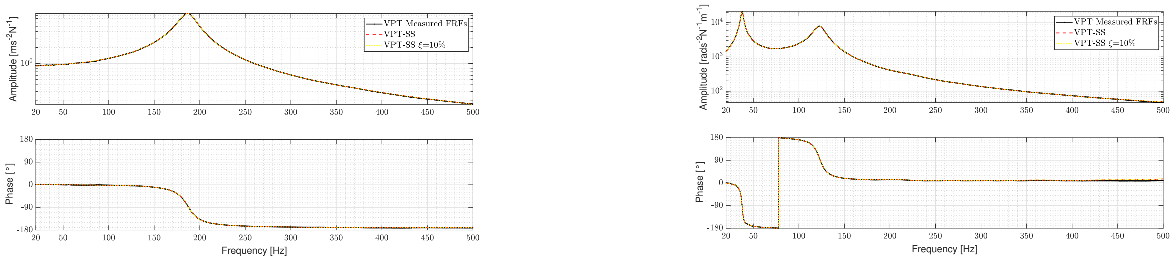

(a) Accelerance FRF of the Assembly Steel, whose output is the DOF v_2^z and the input is the DOF m_1^z.

(b) Accelerance FRF of the Assembly Steel, whose output is the DOF $v_1^{R_y}$ and the input is the DOF $m_2^{R_y}$.

Figure 4: Comparison of the FRFs obtained by applying VPT approach on the measured FRFs (reference FRFs, black) with the same FRFs of the state-space models estimated by using VPT-SS (red) and by including undamped RCMs and RCMs presenting a damping ratio of 10% (yellow).

RCMs and RCMs presenting a damping ratio of 10%.

By observing figures 4, it is straightforward to conclude that all the FRFs well match. This validates the approaches discussed in section 2 to estimate state-space models by including either undamped or damped RCMs.

5 Conclusion

The approaches discussed in this paper showed to be accurate to compute state-space models from experimentally acquired FRFs. Furthermore, the state-space model computed by VPT-SS showed to outperform the state-space model estimated directly from the FRFs obtained by applying the VPT approach to transform the measured FRFs to the intended locations. In fact, it turned out that the model obtained by VPT-SS was composed by a smaller number of states and their FRFs showed to present a better quality match with the FRFs obtained by applying VPT on the measured FRFs, specially at higher frequencies. Nevertheless, the same comparison is recommended to be undertaken with FRFs collected from an experimental modal characterization of different mechanical systems, that in order to better asses the advantage of using VPT-SS.

Acknowledgements

This project has received funding from the European Union's Framework Programme for Research and Innovation Horizon 2020 (2014-2020) under the Marie Sklodowska-Curie Grant Agreement nº 858018.

References

[1] R. Craig and M. Bampton, "Coupling of substructures for dynamic analyses," *AIAA Journal*, vol. 6, no. 7, pp. 1313–1319, 1968.

[2] D. d. Klerk, D. J. Rixen, and J. d. Jong, "The frequency based substructuring (fbs) method reformulated according to the dual domain decomposition method," in 24^{th} *International Modal Analysis Conference*, St. Louis, MO, 2006.

[3] P. Sjövall and T. Abrahamsson, "Component system identification and state-space model synthesis," *Mechanical Systems and Signal Processing*, vol. 21, pp. 2697–2714, 2007.

[4] R. Dias, M. Martarelli, and P. Chiariotti, "Lagrange Multiplier State-Space Substructuring," *Journal of Physics: Conference Series*, vol. 2041, no. 1, p. 012016, 2021.

[5] P. v. Overschee and B. D. Moor, “N4sid: subspace algorithms for the identification of combined deterministic-stochastic systems,” *Automatica*, vol. 30, pp. 75–93, 1994.

[6] P. v. Overschee and B. D. Moor, *Subspace Identification for Linear Systems, Theory - Implementation - Applications*. Kluwer Academic Press, 1996.

[7] T. McKelvey, H. Akcay, and L. Ljung, “Subspace-based multivariable system identification from frequency response data,” *IEEE Transactions on Automatic Control*, vol. 41, pp. 960–979, 1996.

[8] B. Peeters, H. V. d. Auweraer, P. Guillaume, and J. Leuridan, “The polymax frequency-domain method: a new standard for modal parameter estimation?” *Schock and Vibration*, vol. 11, pp. 395–409, 2004.

[9] M. El-Kafafy, B. Peeters, P. Guillaume, and T. D. Troyer, “Constrained maximum likelihood modal parameter identification applied to structural dynamics,” *Mechanical Systems and Signal Processing*, vol. 72-73, pp. 567–589, 2016.

[10] M. El-Kafafy and B. Peeters, “A Robust Identification of Stable MIMO Modal State Space Models,” *In: Dilworth, B.J., Marinone, T., Mains, M. (eds) Topics in Modal Analysis & Parameter Identification, Volume 8. Conference Proceedings of the Society for Experimental Mechanics Series. Springer, Cham*, pp. 81–95, 2023. [Online]. Available: https://doi.org/10.1007/978-3-031-05445-7_10

[11] A. Liljerehn, *Machine Tool Dynamics – A Constrained State-space Substructuring Approach (Doctoral thesis)*, Chalmers University Technology, Götenborg, Sweden, 2016.

[12] T.-J. Su and J.-N. Juang, “Substructure system identification and synthesis,” *Journal of Guidance, Control and Dynamics*, vol. 17, no. 5, pp. 1087–1095, 1994.

[13] M. van der Seijs, D. van den Bosch, D. J. Rixen, and D. de Klerk, “An improved methodology for the virtual point transformation of frequency response functions in dynamic substructuring,” in 4^{th} *ECCOMAS Thematic Conference on Computational Methods in Structural Dynamics and Earthquake Engineering (COMPDYN)*, Kos Island, Greece, 2013, pp. 4334–4347.

[14] F. Lembregts, J. Leuridan, and H. Van Brussel, “Frequency domain direct parameter identification for modal analysis: State space formulation,” *Mechanical Systems and Signal Processing*, pp. 1–17, 1988.

[15] D. Ewins, *Modal Testing: Theory, Practice and Application*. Hertfordshire, England: Research Studies Press Ltd., Second Edition, 2000.

[16] R. Dias, M. Martarelli, and P. Chiariotti, “On the use of Lagrange Multiplier State-Space Substructuring in dynamic substructuring analysis,” *Mechanical Systems and Signal Processing*, vol. 180, 2022. [Online]. Available: https://doi.org/10.1016/j.ymssp.2022.109419

[17] M. Haeussler, S. Klaassen, and D. Rixen, “Comparison of substructuring techniques for experimental identification of rubber isolators dynamic properties,” in *Proceedings of ISMA 2018 - International Conference on Noise and Vibration Engineering and USD 2018 - International Conference on Uncertainty in Structural Dynamics*, Leuven, Belgium, 2018.

[18] M. Haeussler, S. Klaassen, and D. J. Rixen, “Experimental twelve degree of freedom rubber isolator models for use in substructuring assemblies,” *Journal of Sound and Vibration*, vol. 474, p. 115253, 2020.